Pimmer, J., & Holler, E. (1979) *Biochemistry 18*, 3714–3723.
Ramabhadran, T. V., & Jagger, J. (1976) *Proc. Natl. Acad. Sci. U.S.A. 73*, 59–69.
Rupley, J. A., & Gates, V. (1967) *Proc. Natl. Acad. Sci. U.S.A. 57*, 496–510.
Santi, D. V., & Anderson, R. T. (1974) *Anal. Biochem. 58*, 175–182.
Sprinzl, M., & Cramer, F. (1979) *Prog. Nucleic Acid Res. Mol. Biol. 22*, 1–69.
Stuhlberg, M. P. (1967) *J. Biol. Chem. 242*, 1060–1064.
Thomas, G., & Favre, A. (1975) *Biochem. Biophys. Res. Commun. 60*, 1454–1461.
Thomas, G., & Favre, A. (1977) *C. R. Hebd. Seances Acad. Sci., Ser. D 284*, 1345–1347.
von der Haar, F., & Cramer, F. (1978) *Biochemistry 17*, 3139–3145.
Yarus, M. (1972) *Proc. Natl. Acad. Sci. U.S.A. 69*, 1915–1919.

Nuclear Magnetic Resonance and Nuclear Overhauser Effect Study of Yeast Phenylalanine Transfer Ribonucleic Acid Imino Protons†

Paul D. Johnston‡ and Alfred G. Redfield*

ABSTRACT: Results directed primarily toward spectral assignment and nuclear spin dynamics are described for yeast $tRNA^{Phe}$ in 0.1 M NaCl, pH 7. Magnesium titrations were performed. Changes in the spectrum occur for Mg^{2+}/tRNA ratios of about 2 and above 10. Difference spectroscopy between 43 and 29 °C in zero Mg^{2+} concentration, together with prior identification of the GU4 acceptor stem base pair, indicates early acceptor melting and is used to identify acceptor resonances. Transport of spin energy (spin diffusion) is described in tRNA together with a summary of relevant experiments. A survey of nuclear Overhauser effects (NOE's) between imino and aromatic and amino protons is included, together with some recent conclusions based on methyl NOE's and experiments with tRNAs deuterated at the purine C8 position. Assignment of the imino NMR spectrum on the basis of these and previous data is reviewed and discussed in detail. Preliminary distance estimates based on the NOE for AU and GU4 base pairs are in reasonable agreement with the expected distances.

The NMR spectrum of transfer ribonucleic acid (tRNA)[1] provides useful indicators of conformation and dynamics because both the extreme upfield methyl region of the spectrum and the extreme downfield imino region are relatively uncluttered and potentially amenable to assignment. The imino protons are especially interesting (Kearns & Shulman, 1974) because the rates of their exchange with solvent can be measured by NMR in order to obtain information on structural mobility (Crothers et al., 1974; Johnston & Redfield, 1977). Despite much work and progress, assignment of the imino resonance region to specific secondary and tertiary protons is not as complete as is desirable for further applications to biologically relevant problems (Reid & Hurd, 1977; Bolton & Kearns, 1978; Kearns & Bolton, 1978; Patel, 1978; Robillard & Reid, 1979; Schimmel & Redfield, 1980).

This article summarizes our work directed primarily toward assigning the imino region of the spectrum of yeast $tRNA^{Phe}$ on the basis of observations of the nuclear Overhauser effect (NOE) and also on the temperature and magnesium dependence of the spectrum, as well as solvent exchange rates. In a subsequent article, we will present work on the dynamics of unfolding of tRNA measured by NMR. Preliminary publications of this work have appeared (Johnston & Redfield, 1977, 1978), including an introductory exposé (Johnston & Redfield, 1979).

In order to orient our later discussion, we first describe the NMR spectrum at low and moderate temperature as a function of magnesium ion concentration and describe transport of proton spin energy ["spin diffusion"; see Kalk & Berendson (1976)] in tRNA. This is relevant to our observations of the nuclear Overhauser effect in tRNAs as well as to studies of thermal unfolding at higher temperatures.

We then turn to the NOE observations, which tell us unequivocally that pairs of proton resonance lines in the spectrum come from pairs of protons which are adjacent to each other in the structure. Combined with information about the tertiary structure, and NMR experience with model compounds, the NOE can yield new assignments and distance information in favorable cases, and also permits clean resolution of many otherwise obscure NMR lines.

The nuclear Overhauser effect has been described in our earlier papers (Redfield & Gupta, 1971; Johnston & Redfield, 1979). Briefly, it consists of application of a long (0.05–0.5 s) weak preirradiation pulse of radio frequency power at a frequency, f_2, designed to wipe out or saturate a single NMR line at that frequency by pumping energy into the protons resonating at f_2 only. This pulse is followed immediately by an observation pulse, which is especially designed to not excite the strong water resonance. The NMR signal produced by

† From the Department of Biochemistry, Brandeis University, Waltham, Massachusetts 02254. *Received July 1, 1980.* This work was supported in part by U.S. Public Health Service Grants GM20168 and 5T01-GM0212 and by the Research Corporation. This is Publication No. 1335 of the Brandeis University Biochemistry Department. A.G.R. is also at the Physics Department and the Rosensteil Basic Medical Sciences Research Center of Brandeis University.

‡ Present address: Institute of Molecular Biology, University of Oregon, Eugene, OR 97403.

[1] Abbreviations used: tRNA, transfer ribonucleic acid; NOE, nuclear Overhauser effect; EDTA, ethylenediaminetetraacetic acid; T, ribothymidine; m^1A, N^1-methyladenosine; m^2G, N^2-methylguanosine; m^2_2G, N^2-dimethylguanosine; m^7G, N^7-methylguanosine; Ψ, pseudouridine; s^4U, 4-thiouridine.

0006-2960/81/0420-1147$01.25/0

the observation pulse is Fourier transformed, and, with the help of difference spectroscopy, it is found that one or more NMR lines, other than the one directly saturated at f_2, are also saturated. These are lines of protons close (within ~3.5 Å) to the proton resonating at f_2.

Although this paper is mainly concerned with NOE's from the imino to the aromatic and amino regions, we include a few preliminary results involving methyl protons and selectively deuterated tRNA.

We will introduce some of the NMR melting data from our later article. By NMR melting, we mean the apparent disappearance of a line or lines from the spectrum as the temperature is raised. It occurs when the solvent exchange rate of the proton(s) in question reaches about 100 s^{-1} (Crothers et al., 1974). Such data are useful for identification, provided we can assume that melts of related structural elements occur at nearly the same temperature. Finally, we make use of some results on real-time observation of exchange rates at low (15 °C) temperature (Johnston et al., 1979) which suggest identification of one resonance.

These observations support a set of identifications of resonances which differs in some ways from that proposed by Reid, Hurd, and their co-workers (Hurd & Reid, 1979a,b; Hurd et al., 1979; Reid et al., 1979). We will critically discuss these identifications as well as selected proposed alternatives. One interesting aspect of NOE observation of ring-carbon protons is that shifts in their resonances are likely to be relatively simple to interpret since they should be dominated by ring-current shifts. We will discuss these shifts in terms of a predictive scheme (Arter & Schmidt, 1976) based on the assumption of an 11-fold RNA helical structure as an approximation to the tRNA secondary structure.

Materials and Methods

Yeast $tRNA^{Phe}$ was purchased from Boehringer Mannheim and used without further purification, or was purified by DEAE-Sephadex chromatography. Some samples were also purified from unfractionated tRNA (Boehringer Mannheim; Plenum; and also phenol extracted in this laboratory). Preparation and assay procedures are described in detail elsewhere (Johnston, 1979). Only samples with an acceptance of more than 1.6 nmol of Phe/A_{258} unit were used. Dialysis was performed in a microcell with buffers prepared from glass-distilled water, and NMR tubes were acid washed. All buffer chemicals were reagent grade. D_2O (5%) was added to all final dialysis buffers. It had been passed through Chelex before use. All samples contained 0.1 M NaCl and were at pH 7.

One sample, used for the Mg^{2+} titration at 25 °C in the absence of EDTA, was prepared by M. Guéron and J. Leroy. A 20-mg sample of tRNA (Boehringer) was dissolved in 150 mM NaCl and 40 mM triethanolamine buffer, pH 7.4, and passed through two small (6 mm × 1.5 cm) Chelex columns previously neutralized and equilibrated with the same buffer. The final pH was 7.2, and the tRNA concentration was 1.1 mM. Atomic absorption spectroscopy of the sample showed no magnesium, i.e., less than 0.1 Mg^{2+} ion bound per tRNA molecule. Sodium azide, 0.2 mM, was added as a bacteriocide.

NMR spectra were obtained with a 214 observation pulse, to flip over the downfield protons without affecting water protons [Redfield & Kunz (1979) and references cited therein]. The total pulse length was between 0.5 and 0.25 ms. NMR signals were digitized at a rate of 5.12×10^3 or 2.56×10^3 complex points/s, and usually 1024 complex points were obtained per free induction decay. Double irradiation times are given below; for the NOE, these were chosen to approximately equal the time required for a mutual flip between typical neighboring spins. The double irradiation power was usually set empirically to produce about 80% direct saturation with as little direct spillover of saturation to neighboring resonances as possible. Double irradiation was followed by a 2-ms homospoil pulse and a 3-ms spoil-recovery time, before the observation pulse. Most difference spectra were obtained as sets of interleaved block-averaged difference spectra as described elsewhere (Redfield & Kunz, 1979), saving nearly a factor of 2 in running time compared to previous practice.

Results

Spectra vs. Magnesium Concentration. It is well-known that magnesium enhances the stability of tRNA and that, in its absence, fairly high salt concentration is required for it to remain in a form approximating its native state (Crothers & Cole, 1978). We ran all experiments in 0.1 M NaCl and studied the effects of various concentrations of $MgCl_2$. This salt concentration was chosen because it is similar to that used in other studies, and is high enough to prevent nonspecific electrostatic binding (Leroy & Guéron, 1977). Spectra at high and low $MgCl_2$ concentrations are shown in Figure 1, together with the three-dimensional structure of yeast $tRNA^{Phe}$ determined by X-ray crystallography [Quigley et al., 1975; Ladner et al., 1975; reviewed by Rich & RajBhandary (1976); Kim, 1978]. Also shown are the peak labels used by us and the set of possible assignments which we discuss.

Figure 2 shows excerpts from one of two exploratory titrations of spectra as a function of Mg^{2+} concentration, in which we successively added concentrated $MgCl_2$ to a sample and ran spectra after each addition. These titrations were not intended as complete studies of Mg^{2+} binding but were made primarily to give some idea of the Mg^{2+} sensitivity of different spectral lines. The first such titration, presented in detail elsewhere (Johnston, 1979), was performed on a sample that was initially extensively dialyzed against 0.1 M NaCl, 10 mM EDTA, and 10 mM sodium cacodylate, pH 7. Spectra were run at 37 °C. Solvent exchange rates of several protons were measured in this run, and these will be presented and discussed in a later paper. A second titration was performed at 25 °C, in collaboration with M. Guéron and J. Leroy, on a commercial (Boehringer) sample which was in 0.15 M NaCl and 40 mM triethanolamine buffer at pH 7.2, with no initial added EDTA. No exchange rate data were taken from this titration, but data were taken for a greater number of Mg^{2+} concentrations.

The results of these two titrations were consistent with previous studies (Bolton & Kearns, 1977) and were similar to each other. The major differences were the following: (1) As expected, at 37 °C, apparent intensity is missing at zero Mg^{2+} concentration, relative to high Mg^{2+} concentration, at several peaks of the spectrum because these peaks contain resonances of protons which are solvent exchange broadened in the absence of Mg^{2+} and at high temperature. These are peaks F, J, and K, and possibly intensity at peaks O and P. In several cases, this kinetic broadening is expected from our exchange rate data at constant Mg^{2+} concentration (Johnston & Redfield, 1977) and was used to help assign resonances to tertiary protons or terminal helix Watson–Crick imino protons. (2) In the presence of EDTA, spectral changes occur at somewhat higher levels of total added Mg^{2+}, as expected from competition by EDTA for the ion. However, the effect of EDTA is not dramatic.

Both titrations show changes for at least two ranges of the ratio Mg^{2+}/tRNA. First, as this ratio is increased from 0 to slightly more than 2, peak B moves downfield to coalesce with peak A (Figure 2b). A plot of the inverse of the splitting

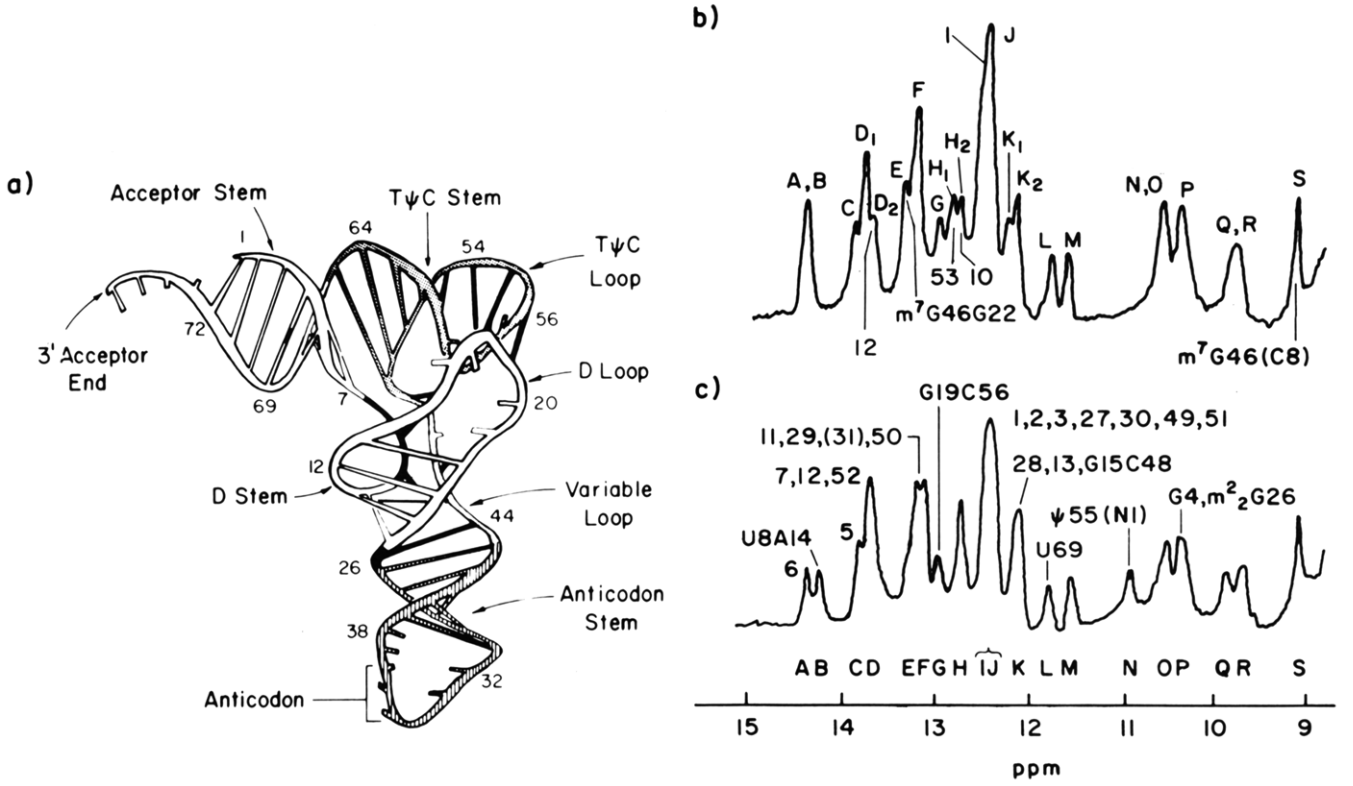

FIGURE 1: (a) Three-dimensional structure of yeast $tRNA^{Phe}$. [Reproduced from Quigley et al. (1975) with permission. Copyright 1975, National Academy of Sciences.] Tertiary interactions are darkened. (b) NMR spectrum at 37 °C in 30 mM $MgCl_2$, 10 mM EDTA, and 0.1 M NaCl. (c) NMR spectrum at 23 °C in zero $MgCl_2$ concentration; other conditions are unchanged. The peaks are lettered as referred to in the text. The set of assignments discussed is also given. Many of these are tentative, as discussed in the article. Secondary proton assignments are denoted by a number which is the first residue of the pair in the sequence. The resonance of AΨ31 is postulated to be the extra intensity in peak F, in spectrum (b). Chemical shifts are downfield relative to sodium 5,5-dimethyl-5-silapentane-2-sulfonate.

between peaks A and B vs. the inverse of added Mg^{2+} concentration appears to be roughly linear for the 25 °C titration in the absence of EDTA. This splitting is reduced by 50% for a Mg^{2+}/tRNA ratio of about 2, both at 25 °C without EDTA and at 37 °C with EDTA. An obvious, but not unique, explanation of this behavior is that there is one strong binding site in competition with several weaker binding sites and that all these sites bind Mg^{2+} more strongly than does EDTA.

A second change which occurs over a range of 4 to about 10 Mg^{2+} per tRNA is the appearance of a shoulder D_2 on peak D (Figure 2c). This shoulder is of considerable interest because the proton responsible for it exchanges with solvent unusually slowly below 20 °C at high Mg^{2+} concentration [in about 24 h; see Johnston et al. (1979)].

Finally, for a ratio range of 10–30 Mg^{2+} per tRNA, there are several obvious changes (Figure 2d). Peak N moves dramatically into peak O–P, and peaks H and K split. New intensity appears between peaks I and J, and they appear to move together. This transition is EDTA dependent and presumably results from near saturation of tRNA with Mg^{2+}, and the appearance of some free Mg^{2+}. The EDTA dependence seems consistent with competition for Mg^{2+} between EDTA and weak binding sites on the tRNA. It is not entirely clear at this writing whether the changes described in the present paragraph really occur at different Mg^{2+} concentration than does the appearance of the shoulder D_2 described above.

Magnetic Transport of Proton Spin Energy. We now summarize the major features of spin-energy transfer via magnetic interaction at low temperature in tRNA. These ideas are by now generally recognized to be applicable to proteins (Kalk & Berendson, 1976; Stoesz et al., 1978); tRNA differs only qualitatively, in having a more open and less multiply connected structure. What follows would be important to recognize in undertaking or evaluating any dynamic NMR experiment in tRNA. Since we have published a preliminary report (Johnston & Redfield, 1978), we will be brief. Extensive details are given elsewhere (Johnston, 1979).

At room temperature, we find that presaturating any part of the spectrum with broad-band frequency-modulated power saturates the rest of the spectrum to a variable degree, in both H_2O and D_2O solvent. Saturating the H_2O resonance produces general disappearance of both exchangeable and nonexchangeable tRNA protons at room temperature; previously, this saturation transfer was misinterpreted as a chemical kinetic effect of solvent proton exchange (Johnston & Redfield, 1977; Campbell et al., 1977). We have found that the relaxation rate of one exchangeable proton depends on the ratio of H_2O to D_2O in the solvent, being shorter in higher H_2O concentration (Johnston & Redfield, 1979). In D_2O, we find that broad-band presaturation of the sugar region completely saturates the methyl region; control experiments show that this is definitely not an artifact due to direct methyl saturation. Recovery from pinpoint saturation occurs in 0.05–0.2 s for most individual resonances, and in 0.1–0.3 s for methyl resonances. On the other hand, recovery from broad-band saturation of a large portion of the spectrum, such as the sugar region (in D_2O), takes on the order of 2 s. This includes the methyl resonances that are not directly saturated.

This body of data is consistent with the NMR behavior of proteins of similar size: individual protons (or methyl protons) exchange magnetization with their nearest neighbors in about 0.1 s on the average. This magnetization thus diffuses among spins rapidly compared to the average time for the magnetization to be dissipated to the lattice (about 2 s). The latter dissipation presumably takes place via interspin dipolar interaction in D_2O; in H_2O, on the other hand, dissipation also

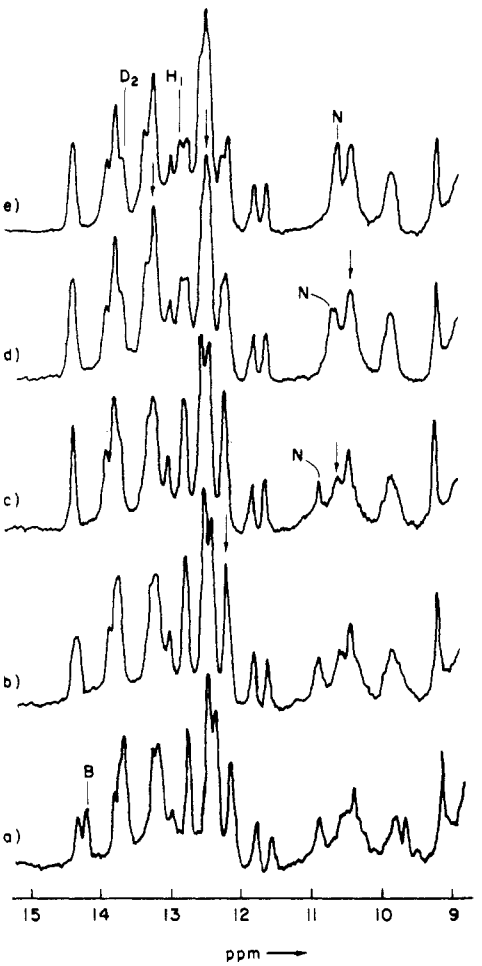

FIGURE 2: Spectra of the imino region of yeast $tRNA^{Phe}$ vs. added concentration of $MgCl_2$ at 37 °C in 0.1 M NaCl, 0.1 M cacodylate buffer, and 10 mM EDTA, pH 7. (a) Metal ions rigorously removed by dialysis. (b–e) Approximately 4, 10, 20, and 30 mM total $MgCl_2$ added. In the presence of $MgCl_2$, spectra are essentially temperature independent below 45 °C. Spectra of samples dialyzed against 5 mM $MgCl_2$ are similar to (e). Arrows indicate places where intensity appears as a result of adding $MgCl_2$. Several peaks which shift with $MgCl_2$ concentration are also labeled as in Figure 1. Transfer RNA concentration was approximately 1 mM.

occurs by magnetic coupling to slowly exchanging (in the range 10^2–10^9 s^{-1}) water protons bound to the tRNA. This picture is reasonable on the basis of standard relaxation theory (Kalk & Berendson, 1976; Noggle & Schirmer, 1971), assuming an overall correlation time of about 10^{-8} s (Komorowski & Allerhand, 1974), except that it is necessary to assume some high-frequency internal motion to explain the overall average relaxation rate of about 0.5 s^{-1} observed by broad-band saturation recovery. We believe that a previous study of methyl relaxation by Davanloo et al. (1979), using a short 90° saturation pulse, measured the average relaxation of a neighborhood of protons near each methyl group; thus, the conclusions drawn about methyl dynamics in that paper were invalid.

Nuclear Overhauser Effects. Transfer of saturation effects between resolved nuclear resonances, resulting from mutual spin flips of the type just discussed, is sometimes called negative NOE because they are indeed a straightforward manifestation of the NOE (Noggle & Schirmer, 1971) but for the special case of a macromolecule for which $\omega\tau \gg 1$ and for which, therefore, the sign of the NOE is opposite to that in small molecules, between protons, or between a proton and a ^{13}C spin (Bothner-By, 1979).

It was suggested by others that NOE's in macromolecules might be uninformative because energy might diffuse among many spins, producing many confusing NOE's. This was not a problem for two reasons: First, tRNA has a fairly open structure so that a given proton is close to only a few other protons, and these are of different classes, having well-separated resonances. Relaxation at the surface by H_2O may also prevent widespread spin diffusion. Second, in the interest of pulsing as often as possible, we applied preirradiation for a relatively short time (100–300 ms), long enough for only one or two mutual spin flips to occur.

Nevertheless, there is the possibility that NOE's involving multiple flips occur, and these have definitely been observed in a protein and are quite interesting (Stoesz et al., 1979). We believe that most of the NOE's reported here are first-order effects involving a single mutual spin flip between the saturated spin and a near neighbor. Such NOE's are generally less than 40%, so that the second-order NOE's should be roughly ≈15% $(0.4)^2$, or less. Most of the NOE's reported here are above the level of 15%.

Since the rate of mutual spin flips, and thus the size of the NOE, varies as the inverse sixth power of the interspin distance, it is obvious that the size of the NOE can be used to extract distance information. Doing so quantitatively requires either that the relaxation time of the nonsaturated nucleus be known or that measurements of the NOE be performed as a function of the preirradiation time. We will discuss distance estimates later, but we have not attempted a serious study of distances in this paper. It is likely that nearly all the NOE's presented here are between neighboring protons on the same base pair. Examination of a tRNA model shows that the sixth power of the distance between such protons is likely to be much less than the sixth power of the distance between protons on different base pairs.

We have shown some examples of NOE's in tRNA in our previous papers. Figure 3 shows an example of a high-resolution survey of two composite lines in the spectrum, yielding NOE action spectra. This experiment effectively resolves individual lines because of its two-dimensional character. Table I shows all the NOE's we found from irradiating the imino region, for three Mg concentrations.

There are six NOE's from the AU imino region below 13 ppm to the aromatic region which are unusually narrow (≤25 Hz), and these are almost certainly carbon protons, since the lack of a nuclear spin on carbon results in a narrow line. These NOE's must, therefore, come from secondary AU and AΨ base pairs or one of the two reverse Hoogstein base pairs (T54–m^1A58 or U8–A14), or the m^7G46–G22 interaction. In the latter three tertiary interactions, there is a purine C8 proton next to an imino proton which is between two rings while for secondary AU base pairs there is an adenine C2 proton next to the imino proton [Kim (1978) and references cited therein]. The two lines in this region which are Mg sensitive (lines D_2 and B at 14.2 and 13.82 ppm at zero Mg concentration, moving to 14.35 and 13.66 ppm at high Mg concentration) show no definite NOE larger than about 10%, but we stress that there could be small, sharp C2 or C8 NOE's which are obscured by the larger but broader amino NOE's which occur in the same region, or which coincide in the aromatic region, with NOE's from lines in the imino region that are close to the lines which show no obvious NOE. As mentioned below, there may be such an NOE from peak B. Another NOE (from 13.2 to 6.85 ppm) is unusually strong and broadens in zero Mg^{2+} concentration, so we believe it may be an overlap of two NOE's.

We have grown purine-requiring cells on C8-deuterated adenine and extracted tRNA from them in order to test which

Table I: Summary of NOE Data[a] from the Imino Region to the Imino-Amino-Aromatic Region

peak irradiated[b]			irradiated position (PPM)[c]			NOE position (PPM)[e]			fractional transfer[f]			line width (Hz)[g]			tentative assignment[h]
Z	L	H	Z	L	H	Z	L	H	Z	L	H	Z	L	H	
A	A (+B)	A (+B)	14.35	14.35		7.73	7.75		0.3	0.7		15	15		UA6
C		C	13.8		13.88[d]	7.84		7.84	0.3		0.5	15		15	AU5
D		D_1	13.8		13.82[d]	7.37[f]		7.33	0.3		0.4	15		15	UA52
D		D_1	13.8		13.79	7.47		7.45	0.3		0.4	15		15	UA7
E + F	E		13.2	13.34		7.15[f]	7.18		0.2	0.2		18	15		AU29
E + F	F		13.2	13.18		6.81	6.85		0.8	0.9		25	17		UA50
E + F	E + F		13.2	13.25		7.8	7.82		1.1	0.9		B	B		
	F			13.18			8.42			0.1			40		
G			12.9												
H	H		12.77	12.77		8.81	8.79		0.2	0.2		40	40		GC10
I + J	I + J		12.45	12.45		8.43	8.41		0.7			B	VB		
I + J	I + J		12.45	12.45		7.85	7.85		2.2			B	VB		
I + J	I + J		12.45	12.45		6.67	6.66		0.6			B	VB		
K	K		12.18	12.15		8.36	8.39		0.5			B	B		
K	K		12.18	12.15		7.88	7.86		1.4			B	B		
K	K		12.18	12.15		6.84	6.83		0.3			B	B		
K	K		12.18	12.15		6.66	6.67		0.2			B	B		
L	L		11.78	11.78		10.41	10.44		0.2	0.2		30	35		U69
M			11.57												
N	N		10.93	10.85		7.35	7.33		0.25	0.3		30	25		Ψ55 N1
O (+P)			10.56	10.6		7.85	7.78		0.5			~40			
O (+P)			10.56	10.6		7.65						~40			
O (+P)			10.56	10.6		7.35						~40			
O (+P)			10.56	10.6		7.05	6.74					~40	~40		
O (+P)			10.56	10.6		6.71	6.28		0.3			~40	25		
P			10.43				7.84						~30		
P			10.43			7.78	7.71					B	~30		
P			10.43	10.42		11.78	11.80		0.2			~30	~30		G4
Q			9.8			none									
R			9.65			none									

[a] Conditions: Z, zero $MgCl_2$ concentration; L, 10 mM added $MgCl_2$; H, 30 mM added $MgCl_2$. All 1 mM tRNA, 10 mM EDTA, 10 mM sodium cacodylate, (pH 7), and 0.1 M NaCl, 20 °C. [b] Letters refer to peaks labeled in Figure 1. [c] Position of irradiated line in downfield from sodium 5,5-dimethyl-5-silapentane-2-sulfonate (DSS). This is the actual irradiation frequency except as noted in footnote *d*. [d] Position of line estimated from fine-grain action spectrum as in Figure 2. [e] Peak position of observed NOE line in downfield from DSS. [f] Estimated area of NOE line divided by estimated area of a resolved single-spin line. In cases where lines are not resolved, it was assumed that relative saturation was the same as for resolved peaks. Transfers greater than 1 are presumably several coincident NOE's. When NOE's are reported but no entry is given here, transfer was at least 0.2 but could not be estimated meaningfully. [g] Full width at half-maximum. B means >40 Hz; VB means >80 Hz. [h] Discussed later in text. Only assignments based on NOE data are included. See Figures 1 and 4 and Table II for other assignments.

of these NOE's are due to secondary AU pairs, and which are due to reverse Hoogsteen pairs or the m^7G46–G22 interactions. This work is reported in detail elsewhere (Sanchez et al., 1980). The mutant used is blocked early in the purine biosynthetic pathway so that all purines should be C8 deuterated. We find that several NOE's are missing in these samples, from methyl peaks, including, for example, one at 2.44 ppm previously assigned to m_2^2G26, to a carbon proton at 8.4 ppm which we assign to the C8 proton of m^2G10. This indicates that label is retained in the tRNA. No NOE in Table I is missing, indicating that none of them can be assigned to m^7G46–G22, U8–A14, or T54–m^1A58, all of which have purine C8 protons adjacent to imino protons. There is no conflict of this result with the previous assignments of Hurd & Reid (1979a) for the m^7G46 imino resonance to peak E. This peak contains several overlapping resonances, two of which show sharp NOE's which remain upon C8 deuteration and are therefore secondary AU resonances. The m^7G46 imino resonance presumably accidentally coincides with these, and the G22 C8 proton is presumably too far away from the imino proton to produce a measurable NOE.

There is also no conflict with previous assignments of peak B as a reverse Hoogsteen peak since we find no strong NOE from it in either labeled or unlabeled tRNA. There is a serious conflict for peak A, which has also been assigned to one of the reverse Hoogsteen imino protons (Hurd & Reid, 1979a; Johnston & Redfield, 1977, 1978) but which must be a secondary AU proton since its sharp NOE to the aromatic region remains in the C8-deuterated sample. The candidates for the two reverse Hoogsteen peaks are peak B, possibly peak D_2, or peaks upfield of peak E, because no sharp NOE's are seen from these peaks to the aromatic region. Peak D_2 was previously observed to exchange very slowly with solvent, in many hours at 15 °C in the presence of magnesium (Johnston et al., 1979), and was tentatively assigned to UA12.

The latter assignment is now considerably bolstered by the finding of a similar peak in *E. coli* $tRNA^{Val}$ at 13.6 ppm, which exchanges in about 1 day at 15 °C in the presence of Mg^{2+}, and the lack of such a peak in yeast $tRNA^{Ala}$ (N. Figueroa, V. Sanchez, and J. S. Tropp, unpublished experiments). The latter species does not contain an AU pair at position 12 while *E. coli* $tRNA^{Val}$ does and has a D-stem structure similar to that of yeast $tRNA^{Phe}$. The three species have similar sequences in the TΨC and D loops, so that the T54–A58 imino proton ought to have similar properties, inconsistent with these slow exchange data and possible assignment of this proton to peak D_2.

Recently, we have found a weak (~10%) NOE from peak B to 7.74 ppm in zero Mg^{2+} concentration which we do not find in the C8-deuterated sample in the same buffer. This observation provides positive support for assigning peak B to a reverse Hoogsteen imino proton such as that of U8–A14, but it must be viewed tentatively since the NOE spectrum (not shown) is of low quality. Because peaks A and B are close

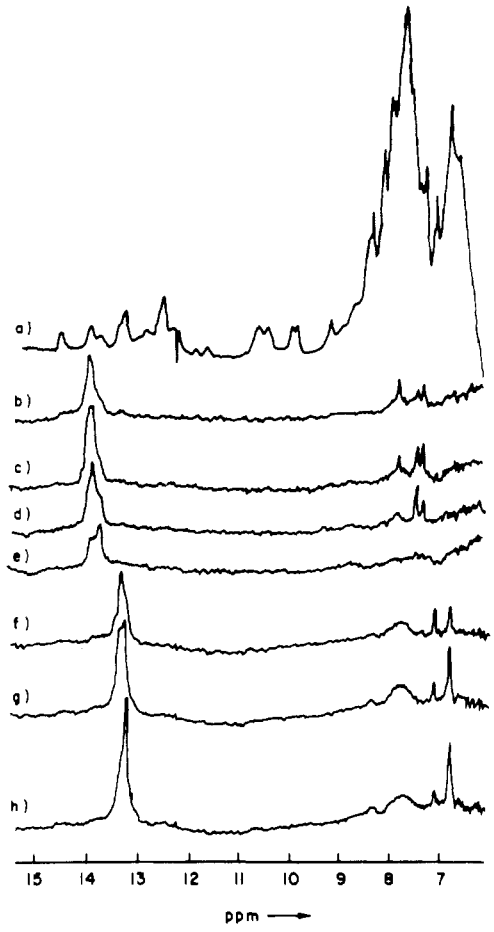

FIGURE 3: Fine-grained NOE survey of composite peaks of the yeast $tRNA^{Phe}$ spectrum at 20 °C in 30 mM added $MgCl_2$; other conditions as in Figure 1. (a) Control spectrum, no irradiation within the spectrum. (b–h) Difference spectra between a control spectrum and spectra obtained with preirradiation at 13.88, 13.82, 13.79, 13.66, 13.34, 13.25, and 13.18 ppm. Preirradiation time 300 ms.

to each other, we placed the control frequency (addition) and peak B irradiation frequency (subtraction) symmetrically about peak A to cancel spillover saturation effects on peak A (Redfield & Kunz, 1979). We have also seen weak NOE's in the same sample, from peaks L and P, previously assigned to GU4 (Johnston & Redfield, 1978), to 13.88 and 7.84 ppm. These NOE's suggest that the latter are resonances of the imino and adenine C2 protons of AU5. Again, this conclusion is highly tentative. We have found no other NOE's that appear to connect protons on different base pairs other than methyl NOE's (below).

NOE's involving the methyl resonances of various tRNAs are being intensively studied in our laboratory (J. Tropp, V. Sanchez, and A. Redfield, unpublished experiments) and will be presented elsewhere. We conclude that the previous assignments (Davanloo et al., 1979) of the methyl resonances of m^2G10, m^7G46, and m_2^2G26 are probably correct. The following conclusions from these studies are relevant to the downfield region. (1) The methyl resonance at 2.75 ppm shows a downfield NOE at 12.63 ppm (peak H_2) which we assign to the m^2G10 methyl to imino NOE. (2) We observe an NOE from 3.8 to 9.17 ppm (peak S) which is the expected NOE from the methyl to the C8 proton of m^7G46. (3) There is a strong NOE from a large methyl resonance at 2.45 ppm, to 10.4 ppm (peak P), which we assigned to the dimethyl and the imino protons of m_2^2G26. (4) From the study of a pattern of NOE's involving the T54 methyl proton, we assigned the previously reported NOE, from 10.93 (peak N) to 7.35 ppm

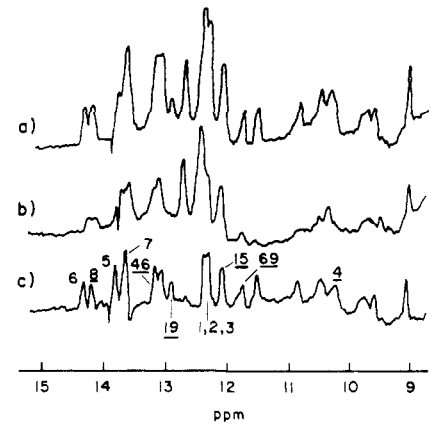

FIGURE 4: (a and b) Zero Mg^{2+} concentration spectrum of yeast $tRNA^{Phe}$ at 20 and 43 °C, respectively. (c) Difference between (a) and (b). The relevant assignments from Figure 1 are marked on the difference spectrum. Secondary protons are marked as in Figure 1, while tertiary protons are underlined, and numbered according to the base donating the imino proton.

(in zero Mg^{2+} concentration), to the N1 and C6 protons of Ψ55 (Tropp & Redfield, 1981).

It is our working hypothesis consistent with observations on several tRNAs that much of the NMR intensity in the region from 9 to 12 ppm is due to imino protons of unpaired bases. These protons would be unobservable in the free base. We assume that the imino proton of m_2^2G26 resonates in this region because steric or stacking interactions disrupt the possible N–H–N interaction with A44; this base pair is characterized as nonplanar by crystallographers (Kim, 1978). Resonances of imino protons in DNA hairpin loops have recently been observed at 10–11 ppm by Haasnoot et al. (1980).

Differential Thermal Spectroscopy. The temperature variation of the spectrum will be discussed in more detail in the following article. Here, we show only one set of results in zero Mg concentration which aids in identification (Figure 4). There are very minor changes in the spectrum between 20 and 35 °C, but at about 38 °C, there are fairly sudden marked changes which coincide with the beginning of the major transition inferred from differential scanning calorimetry in 150 mM NaCl and zero Mg^{2+} concentration (Hinz et al., 1977). Spectra at 29 and 43 °C, and the difference between them, are shown in Figure 4. Because all resonances, including the deuteron lock resonance, shift with temperature, it was necessary to shift the spectra relative to each other to get the difference spectrum, and we show the result of such a frequency shift which yields the best looking difference spectrum in the GC region. No other adjustments of the data were made. Assignments of peaks of the difference spectrum are marked and are the same as in Figure 1. They will be discussed later.

The object behind such studies is to use the fact that resonances which come from protons that exchange in less than about 10 ms, at the high temperature, will be so obscured as a result of kinetic broadening that they will be effectively missing from the spectrum (Crothers et al., 1974). Thus, the difference spectra should highlight resonances of protons which have started to exchange rapidly at the higher temperatures.

Difference spectra of this type should not be overinterpreted. For example, in Figure 4c, there is a negative peak at about 13.7 ppm which apparently arises because a part of the peak at 13.8 ppm moves slightly upfield with temperature. The large peak at about 13.8 ppm in Figure 4c, therefore, does not represent as large a net loss of intensity as it appears. Other peaks in Figure 4c may be distorted similarly.

We note the following: Resonances B and L at 14.2 and 11.78 ppm both are largely gone at 43 °C. These resonances are assigned, respectively, to a tertiary resonance and to the GU4 secondary resonance in the acceptor stem. Therefore, if we are to assume that there is some degree of recognizable organization in the melting of tRNA, it is likely that the acceptor stem and tertiary structure both melt at about 40 °C (or at least have a mean lifetime between transient melting events of about 10 ms at this temperature). We will discuss these assumptions in more detail elsewhere, but now we note that the difference spectra are more consistent with the assumption of early melting of the acceptor stem than with any other analogous assumption in the sense that about the same number of NMR lines have melted in the AU region of the spectrum (~13–15 ppm) as in the GC region (~11–13 ppm), consistent with the equal number of these two types of base pairs in the acceptor stem, and inconsistent with the assumption of melting of the other stems, all of which are GC rich.

Discussion of Assignments

We now consider assignments of the resonances to protons in the structure, and their reliability. Figure 1 shows the set of assignments we will discuss. These follow the assumptions of Reid and co-workers, with a few important modifications and additions.

Reverse Hoogsteen Base Pairs. The resonance positions of these two imino protons (U8–A14 and T54–m^{1}A58) are important since they are interesting tertiary markers. Hurd & Reid assign the two lowest field resonances to them, and thereby are able to explain the positions of all the secondary AU base pairs in several tRNAs by using the ring-current shift theory of Arter & Schmidt and an intrinsic AU position of 14.35 ppm. We have also made the same assignment (Johnston & Redfield, 1979). These assumptions have been questioned by Bolton & Kearns (1978), who prefer an intrinsic position of 14.5 ppm for secondary AU base pairs.

We assign peak B to the imino proton of U8–A14, in agreement with the consensus of previous workers. The basis for this assignment is that a resonance appears in the region of peak B for several *E. coli* tRNAs when s^{4}U8 is dethiolated [Hurd & Reid (1979a) and references cited therein]. In addition, we have found a tentative C8 NOE for peak B, as mentioned above. We do not have a useful assignment for T54–m^{1}A58 at this writing; it is upfield of peak E according to our current assignment.

Other Tertiary Resonances. The imino proton of m^{7}G46 which participates in base pairing with G22, and its C8 proton, has been assigned to peaks E and S at 13.2 and 9.17 ppm, respectively, on the basis of chemical excision of m^{7}G46 (Hurd & Reid, 1979b). We have confirmed the assignment of the C8 proton by the NOE from the m^{7}G46 methyl proton at 3.8 ppm and by real-time exchange studies (Johnston et al., 1979), but we have not found the expected narrow NOE from the imino proton of m^{7}G46 to the C8 proton of G22. The narrow NOE from 13.2 ppm (in zero Mg concentration) to 7.15 ppm is presumably not from this base pair because it remains after purine C8 deuteration. This NOE presumably comes from a secondary AU base pair, and the m^{7}G46 imino resonance accidentally coincides with the AU imino resonance that shows the NOE. This is consistent with our NOE study of *E. coli* tRNA^{Val} (unpublished experiments) where we find no definite narrow NOE to the aromatic region from the resonance assigned by Hurd & Reid (1979b) to the m^{7}G46 imino proton. The latter resonance is better resolved in *E. coli* tRNA^{Val} than in yeast tRNA^{Phe}. Presumably, the distance from the m^{7}G46 imino proton to the G22 C8 proton is unusually large (≳3.5 Å; see below).

The imino resonance of G15–C48 has been assigned by Reid (personal communication) to peak K at 12.1 ppm on the basis of paramagnetic ion broadening (Hurd et al., 1979) and because this peak exchanges more rapidly at a lower temperature, in zero Mg^{2+} concentration, than any nearby peak (Johnston & Redfield, 1979). A portion of this resonance is broadened out of the 37 °C spectrum in zero Mg^{2+} concentration (Figure 2a), but the missing intensity returns upon addition of Mg^{2+} (Figure 2b). We have assigned resonance G at 13 ppm to the G19–C56 Watson–Crick interaction primarily on the basis of its relatively rapid exchange rate in zero Mg concentration at moderate temperature (Johnston & Redfield, 1977); this assignment remains highly tentative. The highly Mg-sensitive peak N at 10.9 ppm (in zero Mg^{2+} concentration) is now assigned to the Ψ55 N1 proton with high reliability, on the basis of NOE studies involving the methyl proton of T54 (Tropp & Redfield, 1981). We previously published the NOE from this peak (Johnston & Redfield, 1978), but it was tentatively assigned to other protons in the structure. We have not found NOE candidates for the amino protons of A9 and A23, or the expected G15 imino–amino NOE, some of which might be expected between 9 and 12 ppm. We now have excellent methyl NOE evidence that the imino proton of m$^2_2$G26 resonates at 10.4 ppm (peak P), instead of around 12.5 ppm as might be expected if it is hydrogen bonded between two planar bases.

The imino protons of G4 and U69 were previously assigned by us to the NOE couple at 10.4 and 11.8 ppm, respectively, on the basis of their uniqueness within the downfield region, model studies, and comparative NOE studies of other tRNAs. This assignment has been bolstered by studies in other tRNAs, and by a ring current shift calculation of Geerdes & Hilbers (1979). Our assignment of the individual G and U imino protons is guided by the latter theory.

Secondary GC Protons. Resonances in the cluttered GC region from 12 to 13.1 ppm are assigned by us mainly on the basis of the previously mentioned ring-current approach of Arter & Schmidt and Hurd & Reid, and Table II compares these assignments with this theory. Further evidence for the assignments of GC1, -2, and -3 comes from their early exchange as the temperature is raised (Figure 3). There is an unusually rapidly exchanging component of peak I (Figure 1), as observed by the saturation-recovery method (Johnston & Redfield, 1979). This component may be due to GC1, which might exchange rapidly because of end fraying. The GC10 imino proton is identified fairly positively as occurring at 12.63 ppm (peak H_2), on the basis of the NOE mentioned above, from a methyl resonance at 2.75 ppm, previously identified with the m^{2}G10 methyl group (Davanloo et al., 1979). Peak H_1 is assigned to GC53 because this residue might be subject to end-fraying effects, and we find that peak H_1 broadens out of the spectrum at 60 °C in the presence of 15 Mg^{2+}/tRNA, somewhat before other GC protons (data not shown).

We have not used any of the broad NOE's observed from the secondary GC region to the aromatic–amino region (Table I) in making assignments. These are presumably imino–amino NOE's. There is not a sufficient body of theory and experiment on the positions of the amino resonances, and they are too broad, to make these NOE's useful. The same applies to imino–amino NOE's from the secondary AU imino region.

Thus, these secondary GC assignments, with the exception of 1–3 and 10, are hardly more than working hypotheses guided by ring-current theory.

Table II: Comparison of Assigned Positions and Ring Current Shift Theory for Secondary Base Pairs

	theory[a]		experiment[b]	
pair	imino	C2	imino	C2 NOE
UA6	13.9	7.92	14.35	7.75
AU5	13.76[c]	7.88	13.88	7.84
UA12	13.78	7.34	13.65[d]	none
UA52	13.67	7.43	13.82	7.33
UA7	13.45[e]	6.97[e]	13.80	7.45
UA50	13.56	7.05	13.2	7.18
AU29	13.55	7.02	13.18	6.85
AΨ31	13.18 ± 0.2[f]	7.88	13.1	none
GC11	13.11		13.18	
CG53	12.48		12.85	
GC10	12.83 ± 0.1[f]		12.76	
CG2	12.7			
GC1	12.5			
GC51	12.46			
GC3	12.46[c]		~12.45	
GC30	12.44			
CG27	12.38 ± 0.1[f]			
CG49	12.33[e]			
CG28	12.10		12.2	
CG13	11.73 ± 0.4[f]			

[a] All values are given in parts per million. Calculated from parameters given by Arter & Schmidt (1976) by using intrinsic imino shifts of 14.35, 13.7, and 13.45 ppm for the AU, AΨ, and GC base pairs, respectively (Reid et al., 1979), and an intrinsic C2 shift of 8.1 ppm (Borer et al., 1975; Kearns, 1976). [b] Line positions (in ppm) observed in the presence of $MgCl_2$. Assignments of these lines to specific base pairs are tentative, as discussed in the text. The AU assignments are more solid than GC assignments with the exception of GC10. [c] Assuming GU4 equivalent to GC. [d] May not be secondary AU. [e] Assuming that the acceptor and T stems stack together as a single RNA 11-fold helix. [f] Calculated shift depends on assumptions concerning shifts by nonsecondary bases, as indicated by ±errors. These do not, of course, reflect the the actual probable errors in the theory, which we have not attempted to evaluate.

Secondary AU Protons. The fact that there are only a small number of secondary AU pairs, and that it is possible to observe NOE's for most of them to C2 protons whose shifts might be nearly predictable from ring-current theory alone, makes this group of resonances appear tractable for identification.

Table II compares theory and experiment for the assignments given in Figures 1 and 4. In general, we have made these assignments to give good agreement with ring-current predictions for the C2 protons. We assume such predictions are reliable for carbon protons but not for imino protons because the electron density around imino protons is likely to depend on details of the geometry, and be different from that for a perfect RNA helix or a hairpin fragment. The following assumptions and reasoning led to these assignments:

(1) AΨ31 is assigned to the resonance intensity at peak F that is missing in zero Mg^{2+} concentration at 20 °C, because this resonance might be susceptible to end-fraying effects (Hilbers et al., 1973; Kearns et al., 1973). However, this assignment remains highly tentative, and AΨ31 could be one of the resonances which shows narrow NOE's.

(2) The acceptor stem melts in zero Mg^{2+} concentration at approximately the same temperature as GU4, which locates the three acceptor AU resonances (Figure 4c).

(3) The most downfield peak A might be a secondary imino proton in an unusual position, i.e., AU5 (next to a GU pair), UA7 (end of helix), or UA12 (involved in tertiary interaction). The base pair UA12 is likely to be stabilized by its tertiary interaction with A9, even in zero Mg^{2+} concentration, and is therefore an unlikely candidate for this relatively labile proton. UA7 is an unlikely candidate for this resonance because the C2 NOE for UA7 is expected more than 1 ppm upfield from where the NOE is found experimentally from the 14.35-ppm peak. This line of reasoning leaves AU5 as the most reasonable candidate for peak A. However, we assign AU5 to peak C on the basis of our recent NOE observation of weak NOE's from the GU4 resonances, peaks L and P, to peak C and its NOE mate at 7.84 ppm. This observation was described above but is not included in Table I because of its preliminary nature. We assign UA6 to peak A on the basis of agreement between the theory for the A67 C2 shift and the experimental NOE from peak A.

(4) Peak D_2 at 13.65 ppm is assigned to AU12 on the basis of the slow exchange experiments described above and previously (Johnston et al., 1979).

(5) The remaining four NOE's are assigned to the remaining four candidates to give good agreement with the C2 ring-current predictions. The agreement between the C2 theory and the observed NOE is worst for UA7 under these assignments, but the predicted position for this C2 proton resonance is most likely to be in error because most of its shift (0.98 ppm) comes from UA6 alone, according to theory, and it is at the end of a standard helix where the structure might be distorted compared to a model helix.

These assignments are highly tentative and are inconsistent with the possibility mentioned above that the NOE from 13.18 to 6.85 ppm may be two overlapping NOE's; on the other hand, the lack of an NOE for UA12 is consistent with the strong variation in NOE's implied by our assignment; possibly, AU base pairs are prone to relatively large variations in geometry.

Further work is desirable to establish these assignments. Comparative studies of other tRNAs at higher field and sensitivity are likely to be useful.

Distance Estimates. Detailed distance estimates will be given elsewhere for selected parts of the structure, together with relevant theory (Tropp, 1980). Here, we briefly consider estimates for the imino–imino distance for the GU pair and the imino–C2 distance for the AU pairs. We have exhaustively studied the relaxation rate of the downfield member of the GU resonance pair (peak L), and it is 7 s^{-1} in 95% H_2O at room temperature. We repeatedly observed the NOE from the upfield member of the two GU resonances (peak P) to peak L, and it is a maximum of about 0.25 of the intensity of a single proton resonance. Thus, the rate of saturation transfer is 0.25×7 s^{-1} or about 2 s^{-1}. Theory states that this rate is $(5.68 \times 10^{10})\tau_c/r^6$. Taking $\tau_c = 2 \times 10^{-8}$, we find $r = 2.88$ Å. Errors in τ_c and in the rate estimate might lead to a 10% distance error. This distance is more than might be expected for the imino–imino proton distance of the GU pair. The latter distance might be nearly the same as the imino–amino distance for a GC pair, or about 2.5 Å [see Figure 4–9 in Bloomfield et al. (1974)]. In a previous paper (Johnston & Redfield, 1978), we stated this distance incorrectly, as was kindly pointed out to us by Dr. Paul Schmidt.

We have not made the required measurements, varying preirradiation times, to accurately estimate the distances for standard AU pairs from the adenine C2 protons to the uracil N3 protons, but a rough estimate is close to the expected 3 Å. A detailed study of distances in the vicinity of the T54 methyl proton will be published elsewhere (J. S. Tropp and A. G. Redfield, unpublished experiments).

Conclusions

The application of nuclear Overhauser effects to tRNA has permitted identification of more NMR lines than has any other method. Largely beyond the scope of this article are NOE

confirmations of several methyl resonances and numerous aromatic protons nearby. Among the imino protons, we have identified both GU protons and that of m_2^2G26, as well as the unpaired N_1 proton of Ψ55. We have tentatively identified the resonance of one of two reverse Hoogsteen base pairs, probably U8–A14, in agreement with earlier workers. Although most secondary base pairs remain unassigned, we have at least been able to enumerate the positions of six out of eight AU and AΨ base pairs, and have a solid identification of GC10.

The six resonance positions we find for the secondary AU pairs are not in good agreement with any prior set of assignments based on ring-current theory; however, our own assignments (Table II) are only slightly more likely to be correct. The resonance position of GC10 is in agreement with the Hurd–Reid–Arter–Schmidt theory, but that of m_2^2G26 was not correctly guessed previously. The most downfield peak A was incorrectly assigned to T54–A58 by Hurd & Reid (1979); assignment of this base pair to the vicinity of 13.8 ppm by Bolton & Kearns was also in error unless our assignment of peak D_2 to UA12, based on slow exchange studies of three tRNA species, is incorrect. We do not disagree with tertiary imino resonance assignments by Hurd, Reid, and co-workers, other than those of T54–A58 and m_2^2G26.

Of the tertiary resonances, the assignment of the Watson–Crick pair G19–C56 seems least solid, which is unfortunate since this base pair, at the outside of the corner of the molecule, might be expected to be most affected by major flexing of the two sections of the molecule. Equally unfortunate, we have no assignment for T54–m^1A58, in the same area of the molecule.

The NMR spectrum of the exchangeable protons of yeast $tRNA^{Phe}$ is now assigned fairly well. As we have indicated, some further experiments may help to confirm these conclusions, or alter them. However, the time has arrived to start to apply this knowledge to obtain an understanding of the dynamics and function of tRNA. A subsequent article will describe our work in this area.

We have made some use of ring-current calculations in our identifications, especially for adenine C2 protons. It would be useful to have predictions for these shifts for different published crystal structures and for different assumed ring currents and, especially, to have an idea of how much these predictions change when sterically reasonable changes are made in the assumed structure.

Acknowledgments

We thank our co-workers, especially Nara Figueroa, James Tropp, and Valentina Sanchez, for help in this work. We thank Drs. H. Geerdes, G. Quigley, and P. Schimmel, and especially Dr. Brian Reid and his co-workers, for information and advice and Drs. M. Guêron and J. Leroy for their collaboration on the magnesium titration.

References

Arter, D. B., & Schmidt, P. G. (1976) *Nucleic Acids Res. 3*, 1437.

Bloomfield, V. A., Crothers, D. M., & Tinoco, I. (1974) *Physical Chemistry of Nucleic Acids*, Harper and Row, New York.

Bolton, P. H., & Kearns, D. R. (1977) *Biochemistry 16*, 5729.

Bolton, P. H., & Kearns, D. R. (1978) *Biol. Magn. Reson. 1*, 91.

Borer, R. N., Kan, L. S., & Ts'o, P. O. P. (1975) *Biochemistry 14*, 1847.

Bothner-By, A. (1979) in *Biological Applications of Magnetic Resonance* (Shulman, R. G., Ed.) p 177, Academic Press, New York.

Campbell, I. D., Dobson, C. M., & Ratcliffe, R. G. (1977) *J. Magn. Reson. 27*, 455.

Crothers, D. M., & Cole, P. E. (1978) in *Transfer RNA* (Altman, S., Ed.) p 196, MIT Press, Cambridge, MA.

Crothers, D. M., Cole, P. E., Hilbers, C. W., & Shulman, R. G. (1974) *J. Mol. Biol. 87*, 63.

Davanloo, P., Sprinzl, M., & Cramer, F. (1979) *Biochemistry 18*, 3189.

Geerdes, H. A. M., & Hilbers, C. W. (1979) *FEBS Lett. 107*, 125.

Haasnoot, C. A. G., den Hartog, J. H. J., de Rooij, J. F. M., van Boom, J. H., & Altona, C. (1980) *Nucleic Acids Res. 8*, 196.

Hilbers, C. W., Shulman, R. G., & Kim, S.-H. (1973) *Biochem. Biophys. Res. Commun. 55*, 953.

Hinz, H. F., Filimonov, V. V., & Privalov, P. L. (1977) *Eur. J. Biochem. 72*, 79.

Hurd, R. E., & Reid, B. R. (1979a) *Biochemistry 18*, 4005.

Hurd, R. E., & Reid, B. R. (1979b) *Biochemistry 18*, 4017.

Hurd, R. E., Azhderian, E., & Reid, B. R. (1979) *Biochemistry 18*, 4012.

Johnston, P. D. (1979) Ph.D. Thesis, Brandeis University, Waltham, MA.

Johnston, P. D., & Redfield, A. G. (1977) *Nucleic Acids Res. 4*, 3599.

Johnston, P. D., & Redfield, A. G. (1978) *Nucleic Acids Res. 5*, 3913.

Johnston, P. D., & Redfield, A. G. (1979) in *Transfer RNA: Structure, Properties, and Recognition* (Abelson, J., Schimmel, P. R., & Soll, D., Eds.) p 191, Cold Spring Harbor Laboratory, Cold Spring Harbor, NY.

Johnston, P. D., Figueroa, N., & Redfield, A. G. (1979) *Proc. Natl. Acad. Sci. U.S.A. 76*, 3130.

Kalk, A., & Berendson, H. J. C. (1976) *J. Magn. Reson. 24*, 343.

Kearns, D. R. (1976) *Annu. Rev. Biophys. Bioeng. 6*, 477.

Kearns, D. R., & Shulman, R. G. (1974) *Acc. Chem. Res. 7*, 33.

Kearns, D. R., & Bolton, P. H. (1978) in *Biomolecular Structure and Function* (Agris, P. F., Ed.) p 493, Academic Press, New York.

Kearns, D. R., Lightfoot, D. R., Wong, K. L., Wong, Y. P., Reid, B. R., Cary, L., & Shulman, R. G. (1973) *Ann. N.Y. Acad. Sci. 222*, 324.

Kim, S.-H. (1978) in *Transfer RNA* (Altman, S., Ed.) p 248, MIT Press, Cambridge, MA.

Komorowski, R. A., & Allerhand, A. (1974) *Biochemistry 13*, 369.

Ladner, J. E., Jack, A., Robertus, J. D., Brown, R. S., Rhodes, D., Clark, B. F. C., & Klug, A. (1975) *Proc. Natl. Acad. Sci. U.S.A. 72*, 4414.

Leroy, J. L., & Guêron, M. (1977) *Biopolymers 16*, 2429.

Noggle, J. H., & Schirmer, P. E. (1971) *The Nuclear Overhauser Effect*, Academic Press, New York.

Patel, D. J. (1978) *Annu. Rev. Phys. Chem. 29*, 337.

Quigley, G. J., Wong, A. H. J., Seeman, N. C., Suddath, F. L., Rich, A., Sussman, J. L., & Kim, S. H. (1975) *Proc. Natl. Acad. Sci. U.S.A. 72*, 4866.

Redfield, A. G., & Gupta, R. K. (1971) *Cold Spring Harbor Symp. Quant. Biol. 36*, 405.

Redfield, A. G., & Kunz, S. D. (1979) in *NMR and Biochemistry* (Opella, S. J., & Lu, P., Eds.) p 225, Marcel Dekker, New York.

Reid, B. R., & Hurd, R. E. (1977) *Acc. Chem. Res. 10*, 396.
Reid, B. R., McCollum, L., Ribiero, N. S., Abbate, J., & Hurd, R. E. (1979) *Biochemistry 18*, 3996.
Rich, A., & RajBhandary, T. (1976) *Annu. Rev. Biochem. 45*, 805.
Robillard, G. T., & Reid, B. R. (1979) in *Biological Applications of Magnetic Resonance* (Shulman, R. G., Ed.) p 45, Academic Press, New York.
Sanchez, V., Redfield, A. G., Johnston, P., & Tropp, J. S. (1980) *Proc. Natl. Acad. Sci. U.S.A. 77*, 5959.
Schimmel, P. R., & Redfield, A. G. (1980) *Annu. Rev. Biophys. Bioeng. 9*, 181.
Stoesz, J. D., Redfield, A. G., & Malinowski, D. P. (1978) *FEBS Lett. 91*, 320.
Stoesz, J. D., Malinowski, D. P., & Redfield, A. G. (1979) *Biochemistry 18*, 4669.
Tropp, J. S. (1980) *J. Chem. Phys. 72*, 6035.
Tropp, J. S., & Redfield, A. G. (1981) *Biochemistry* (in press).

Proton Nuclear Magnetic Resonance Determination of the Sequential Ytterbium Replacement of Calcium in Carp Parvalbumin†

Lana Lee and Brian D. Sykes*

ABSTRACT: The substitution of the paramagnetic lanthanide ion ytterbium for the calcium ions bound to the CD and EF sites of carp parvalbumin results in a series of ^{1}H NMR resonances which are shifted far outside the envelope of the ^{1}H NMR spectrum of the diamagnetic form of the protein. Titrations of Ca^{2+}-saturated parvalbumin with ytterbium (Yb^{3+}) demonstrate that Yb^{3+} sequentially replaces the two bound calcium ions of the protein. Analysis of the ^{1}H NMR data yields the relative affinities of the two sites (CD and EF) for ytterbium with respect to calcium. The dissociation constants for ytterbium are then calculated to be $K_{Yb^{3+}}^{CD} = (4–7) \times 10^{-10}$ M and $K_{Yb^{3+}}^{EF} = (2–6) \times 10^{-10}$ M from the known dissociation constants for calcium [Haiech, J., Derancourt, J., Pechere, J.-F., & Demaille, J. G. (1979) *Biochemistry 18*, 2752–2758]. The approximate equality of these constants is verified by Yb^{3+} titrations of apoparvalbumin.

The X-ray crystallographic structure of the calcium binding protein parvalbumin from carp reveals that each of its two calcium binding sites is completely formed from a contiguous polypeptide sequence folded into the homologous CD and EF hands (Kretsinger & Nockolds, 1973). Each Ca^{2+} binding site contains two turns of helix, a 12-residue loop around the metal, and a second two-turn helix. The loop around the metal contains regularly spaced carboxyl, carbonyl, and hydroxyl ligands. Homologous sequences to parvalbumin (Kretsinger, 1976) can be found in a number of Ca^{2+} binding proteins such as rabbit skeletal troponin C and the myosin alkali light chains (Collins, 1974; Weeds & McLachlan, 1974), the 5,5′-dithiobis(2-nitrobenzoic acid) (DTNB)[1] light chains (Collins, 1976), bovine calmodulin (Vanaman et al., 1977; Stevens et al., 1976), rat testis calmodulin (Dedman et al., 1978), bovine intestinal calcium binding protein (Fullmer & Wasserman, 1977), and the procine intestinal calcium binding protein (Hofmann et al., 1979). The number of times in a given protein the sequence repeats, and the amino acid substitutions therein, can be correlated with the number of metals bound to the protein and their binding strengths, respectively. These findings have led to the proposal that homologous structures, at least at the level of the calcium binding sites, exist for all these proteins.

We have described elsewhere the strategy and development of an NMR methodology whose final goal is the comparison of the structures of calcium binding proteins in solution (Lee et al., 1979; Lee & Sykes, 1980a–d). The technique will enable us to test the hypothesis that all of these calcium binding proteins have homologous structures. The method is based upon the fact that the interaction of calcium binding proteins such as parvalbumin with lanthanides such as ytterbium results in a series of ^{1}H NMR resonances shifted far outside the normal chemical shift range of the diamagnetic form of the protein. These shifted resonances are sensitive monitors of the behavior and geometry of the metal binding sites in solution. Our overall approach is to study carp parvalbumin initially and to use the known X-ray structure of this protein to determine the unknown parameters of the NMR experiment, which are required before the shifts and broadenings can be interpreted in terms of the structure of the protein. With these parameters, and the knowledge of the amino acid substitutions for different proteins, we will then be able to compare the calculated and observed NMR spectra of a new protein as a probe of its structure.

In this paper, we focus on the analysis of the stoichiometry of the binding of Yb^{3+} to carp parvalbumin (p*I* 4.25). We have chosen Yb^{3+} for our study primarily because the contact interaction is the smallest relative to the other lanthanides (Reuben, 1973). In addition, the ratio of the susceptibility line broadening to the pseudocontact shift is relatively small; this results in comparatively high resolution spectra for the shifted peaks (Lee & Sykes, 1980a).

Titrations of Ca^{2+}-saturated parvalbumin with ytterbium demonstrate that there is a sequential replacement of the two protein-bound calcium ions. Analysis of the data allows us to determine, for each of the two sites (CD and EF), the

† From the Medical Research Council Group on Protein Structure and Function and the Department of Biochemistry, University of Alberta, Edmonton, Alberta, Canada T6G 2H7. *Received July 14, 1980.* This work was supported by the Medical Research Council of Canada Group on Protein Structure and Function and the University of Alberta in the form of a dissertation fellowship to L.L.

[1] Abbreviations used: EDTA, ethylenediaminetetraacetic acid; DSS, sodium 4,4-dimethyl-4-silapentane-1-sulfonate; DTT, dithiothreitol; Mes, 2-(*N*-morpholino)ethanesulfonic acid; Pipes, piperazine-*N*,*N*′-bis(2-ethanesulfonic acid); DTNB, 5,5′-dithiobis(2-nitrobenzoic acid); EGTA, ethylene glycol bis(β-aminoethyl ether)-*N*,*N*′-tetraacetic acid; Tricine, *N*-tris(hydroxymethyl)methylglycine; Hepes, *N*-2-(hydroxyethyl)-piperazine-*N*′-2-ethanesulfonic acid.

0006-2960/81/0420-1156$01.25/0